WASA-FRS EXPERIMENTS IN FAIR PHASE-0 AT GSI*

Y.K. Tanaka[a], P. Achenbach[b,c], H. Alibrahim Alfaki[d], F. Amjad[d], M. Armstrong[d,e], K.-H. Behr[d], J. Benlliure[f], Z. Brencic[g,h], T. Dickel[d,i], V. Drozd[d,j,a], S. Dubey[d], H. Ekawa[a], S. Escrig[k,a], M. Feijoo-Fontán[f], H. Fujioka[l], Y. Gao[a,m,n], H. Geissel[d,i], F. Goldenbaum[o], A. Graña González[f], E. Haettner[d], M.N. Harakeh[j], Y. He[a,p], H. Heggen[d], C. Hornung[d], N. Hubbard[d,q], K. Itahashi[r,s], M. Iwasaki[r,s], N. Kalantar-Nayestanaki[j], A. Kasagi[a,t], M. Kavatsyuk[j], E. Kazantseva[d], A. Khreptak[u,v], B. Kindler[d], R. Knoebel[d], H. Kollmus[d], D. Kostyleva[d], S. Kraft-Bermuth[w], N. Kurz[d], E. Liu[a,m,n], B. Lommel[d], V. Metag[i], S. Minami[d], D.J. Morrissey[x], P. Moskal[v,y], I. Mukha[d], A. Muneem[a,z], M. Nakagawa[a], K. Nakazawa[t], C. Nociforo[d], H.J. Ong[n,α,β], S. Pietri[d], J. Pochodzalla[b,c], S. Purushothaman[d], C. Rappold[k], E. Rocco[d], J.L. Rodríguez-Sánchez[f], P. Roy[d], R. Ruber[γ], T.R. Saito[a,d,p], S. Schadmand[d], C. Scheidenberger[d,i], P. Schwarz[d], R. Sekiya[δ,r,s], V. Serdyuk[o], M. Skurzok[v,y], B. Streicher[d], K. Suzuki[d,ϵ], B. Szczepanczyk[d], X. Tang[m], N. Tortorelli[d], M. Venclj[g], H. Wang[a], T. Weber[d], H. Weick[d], M. Will[d], K. Wimmer[d], A. Yamamoto[ζ], A. Yanai[η,a], J. Yoshida[a], J. Zhao[d,θ]

WASA-FRS/Super-FRS Experiment Collaboration

[a]High Energy Nuclear Physics Laboratory, RIKEN Cluster for Pioneering Research, RIKEN, 351-0198 Wako, Saitama, Japan
[b]Institute for Nuclear Physics, Johannes Gutenberg University 55099 Mainz, Germany
[c]Helmholtz Institute Mainz, Johannes Gutenberg University 55099 Mainz, Germany
[d]GSI Helmholtzzentrum für Schwerionenforschung GmbH 64291 Darmstadt, Germany
[e]Institut für Kernphysik, Universität Köln, 50923 Köln, Germany
[f]Universidade de Santiago de Compostela, 15782 Santiago de Compostela, Spain
[g]Jožef Stefan Institute, 1000 Ljubljana, Slovenia
[h]University of Ljubljana, 1000 Ljubljana, Slovenia
[i]Universität Gießen, 35392 Gießen, Germany
[j]University of Groningen, 9747 AA Groningen, The Netherlands
[k]Instituto de Estructura de la Materia — CSIC, 28006 Madrid, Spain
[l]Tokyo Institute of Technology, 152-8550 Tokyo, Japan
[m]Institute of Modern Physics, Chinese Academy of Sciences 730000 Lanzhou, China

[n]School of Nuclear Science and Technology
University of Chinese Academy of Sciences, 100049 Beijing, China
[o]Institut für Kernphysik, Forschungszentrum Jülich, 52425 Jülich, Germany
[p]Lanzhou University, 730000 Lanzhou, China
[q]Institut für Kernphysik, Technische Universität Darmstadt
64289 Darmstadt, Germany
[r]Meson Science Laboratory, RIKEN Cluster for Pioneering Research, RIKEN
2-1 Hirosawa, 351-0198 Wako, Saitama, Japan
[s]Nishina Center for Accelerator-Based Science, RIKEN, 2-1 Hirosawa, 351-0198
Wako, Saitama, Japan
[t]Graduate School of Engineering, Gifu University, 501-1193 Gifu, Japan
[u]INFN, Laboratori Nazionali di Frascati, Frascati, 00044 Roma, Italy
[v]Institute of Physics, Jagiellonian University, 30-348 Kraków, Poland
[w]TH Mittelhessen University of Applied Sciences, 35390 Gießen, Germany
[x]National Superconducting Cyclotron Laboratory, Michigan State University
MI 48824 East Lansing, USA
[y]Center for Theranostics, Jagiellonian University, 30-348 Kraków, Poland
[z]Faculty of Engineering Sciences, Ghulam Ishaq Khan Institute
of Engineering Sciences and Technology, 23640 Topi, Pakistan
[α]Joint Department for Nuclear Physics, Lanzhou University and Institute
of Modern Physics, Chinese Academy of Sciences, 730000 Lanzhou, China
[β]Research Center for Nuclear Physics, Osaka University, 567-0047 Osaka, Japan
[γ]Uppsala University, 75220 Uppsala, Sweden
[δ]Kyoto University, 606-8502 Kyoto, Japan
[ϵ]Ruhr-Universität Bochum, Institut für Experimentalphysik I
44780, Bochum, Germany
[ζ]KEK, 305-0801 Tsukuba, Ibaraki, Japan
[η]Saitama University, Sakura-ku, 338-8570 Saitama, Japan
[θ]Peking University, 100871 Beijing, China

Received 30 November 2022, accepted 15 February 2023,
published online 22 March 2023

We have developed a new and unique experimental setup integrating the central part of the Wide Angle Shower Apparatus (WASA) into the Fragment Separator (FRS) at GSI. This combination opens up possibilities of new experiments with high-resolution spectroscopy at forward 0° and measurements of light decay particles with nearly full solid-angle acceptance in coincidence. The first series of the WASA-FRS experiments have been successfully carried out in 2022. The developed experimental setup and two physics experiments performed in 2022 including the status of the preliminary data analysis are introduced.

DOI:10.5506/APhysPolBSupp.16.4-A27

* Presented at the Zakopane Conference on Nuclear Physics, *Extremes of the Nuclear Landscape*, Zakopane, Poland, 28 August–4 September, 2022.

1. Introduction

The research on exotic hadron–nucleus bound systems is one of the important topics in contemporary nuclear and hadron physics, since they can provide valuable information on hadron properties and interactions particularly in the low-energy region of quantum chromodynamics. Examples of such systems are meson–nucleus bound states (mesic-atoms and mesic-nuclei) and hypernuclei, which have been studied for many decades with various experimental methods and devices [1–9].

We have developed and constructed a new experimental setup integrating the central part of the Wide Angle Shower Apparatus (WASA) [10, 11] into the Fragment Separator (FRS) at GSI [12]. The FRS is a multi-stage magnetic spectrometer at forward 0° with an excellent momentum resolving power up to $\sim 10^4$. The WASA central detector is, on the other hand, a versatile detector system for charged particles and high-energy photons covering a solid angle of nearly 4π. The combination of these two devices enables us to perform simultaneous measurements of forward heavy ejectiles with high momentum resolution and light decay particles with large angular acceptance.

We carried out a first series of the WASA-FRS experiments from January to March 2022 in the framework of the FAIR Phase-0 program at GSI. Two physics experiments, spectroscopy of η'-mesic nuclei with proton beams [13] and of hypernuclei with heavy-ion beams (HypHI experiment) [14], were performed after the commissioning of the entire detector system.

The first experiment aims at observing η'-meson-bound states in carbon nuclei for studying in-medium η'-meson properties. While the existence of such bound states has been theoretically predicted for various cases of η'-nucleus potentials [15–20], no experimental observation was reported so far [21–23]. We performed missing-mass spectroscopy of the ^{12}C(p,d) reaction near the η'-meson production threshold with the FRS and simultaneously detected particles such as protons emitted in the decay of the η'-mesic nuclei with the WASA detector in order to significantly enhance the experimental sensitivity compared to the previous experiment.

In the HypHI experiment, we performed invariant-mass spectroscopy of light hypernuclei with heavy-ion beams. We produced Λ-hypernuclei via projectile fragmentation with the capture of a Λ hyperon, and measured the π^- and the residual nucleus emitted in a mesonic decay mode by the WASA detector and the FRS, respectively. Since the produced hypernuclei are in the projectile frame with a relativistic velocity, reconstructing the decay vertices allows the determination of the lifetime of the hypernuclei. In the first WASA-FRS experiment in 2022, the main goals are set to give answers to the two puzzles raised by the previous HypHI experiments at GSI: indication of a neutral $nn\Lambda$ bound system [24] and a short lifetime of ${}^{3}_{\Lambda}$H [25].

In this contribution, we introduce the WASA-FRS experiments performed in 2022 including the developments for the new experimental setup. Reports from the beam times and preliminary status of the data analysis are presented.

2. Experiment

2.1. Experimental setup and method

A general configuration of the WASA-FRS experiments is represented in Fig. 1. The WASA central detector, additional detectors, and a reaction target are installed at the central focal plane of the FRS (F2). A primary beam from the heavy-ion synchrotron SIS-18 or a secondary beam produced and separated in-flight in the first half of the FRS (TA-F2) impinge on a reaction target at F2. Exotic hadronic systems can be produced in nuclear reactions, and light particles emitted in the decay are detected by the WASA central detector with large angular acceptance. At the same time, particles ejected at 0° forward are unambiguously identified in the second half of the FRS (F2–F4) with a selection of magnetic rigidity by the FRS, and with velocity and energy deposition measured by the plastic scintillators (SC31 at F3 and SC41, SC42, and SC43 at F4). Momenta of the forward particles are obtained with an excellent momentum-resolving power up to 10^4 by measuring their tracks with multi-wire drift chambers (MWDCs) at the dispersive focal plane F4.

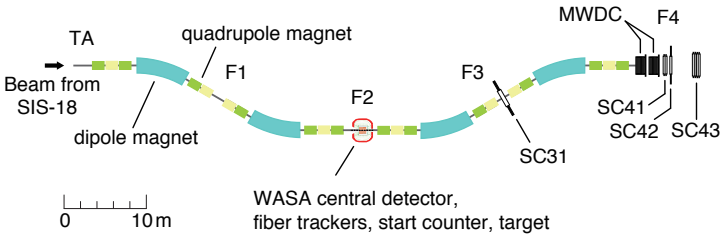

Fig. 1. A schematic view of the general experimental setup integrating the WASA central detector at the fragment separator FRS. See the text for details.

Figure 2 shows the detailed experimental setup at F2 used in 2022. The WASA central detector, consisting of a mini-drift chamber (MDC), a plastic scintillator barrel (PSB), and forward and backward end-caps (PSFE and PSBE, respectively), a superconducting solenoid magnet [26], and a scintillator electromagnetic calorimeter (SEC) were used in common. We adopted the original apparatuses except for the plastic scintillators (PSB, PSFE, PSBE), which we replaced with newly-developed ones, as shown in Fig. 3, equipped with multi-pixel photon counters (MPPC) directly attached to the scintillator bars for achieving a time resolution better than 100 ps (σ) [27].

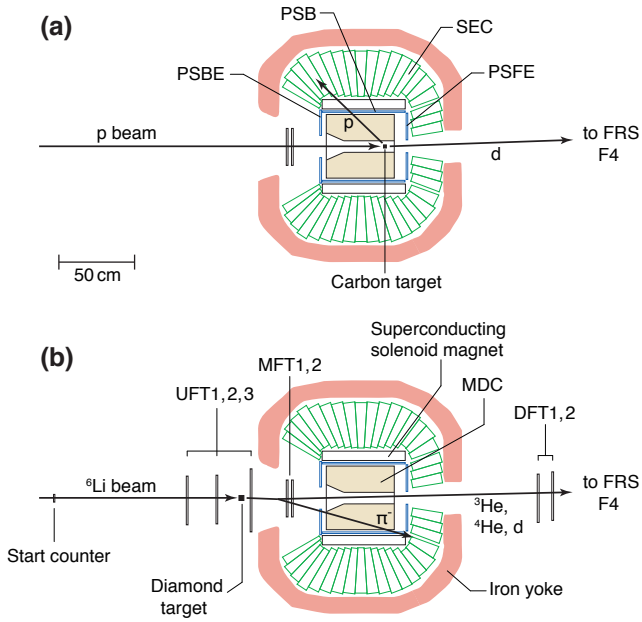

Fig. 2. Experimental configurations at FRS-F2 for the spectroscopy experiment of η'-mesic nuclei (a) and the HypHI experiment (b). See the text for details.

Panel (a) in Fig. 2 shows the schematic setup for the η'-mesic nuclei spectroscopy. A 2.5 GeV proton beam with an intensity up to $\sim 3\times10^8$/s was guided through a hole in the HypHI fiber trackers (MFTs) and impinged on a 4 g/cm^2-thick carbon target installed in the inner beam pipe of the MDC. η'-mesic ^{11}C nuclei can be populated in the ^{12}C(p,d) reaction. Forward-emitted deuterons were identified and momentum-analyzed by the F2–F4 section of the FRS, while decaying particles from mesic nuclei, in particular, protons in backward directions, where we expect a good signal-to-noise ratio, were detected by the WASA system.

The HypHI experiment utilized a different detector configuration at F2, as illustrated in panel (b), due to different kinematics. A 1.96 GeV/u ^{6}Li beam with an intensity of the order of 10^7/s was incident on a 9.87 g/cm^2 diamond target to produce light Λ-hypernuclei via projectile fragmentation followed by the capture of a Λ hyperon in the projectile spectator. Hypernuclei produced in-flight can travel a distance of the order of some 10 cm, and then decay into π^- and forward residues in the case of the two-body mesonic decay. The produced hypernuclei can be identified with the invariant-mass spectroscopy technique by measuring the momentum of the π^- with the WASA detector and that of the forward residue with high momentum resolving power by the FRS. Additional scintillating fiber trackers (UFTs,

MFTs, and DFTs) were installed for measuring all the relevant trajectories to determine the primary reaction vertex and the decay vertex, which are essential to deduce the lifetime of the hypernuclei. In addition, a start counter consisting of segmented plastic scintillators was placed at the entrance of FRS-F2 to define the start timing of the time-of-flight measurements.

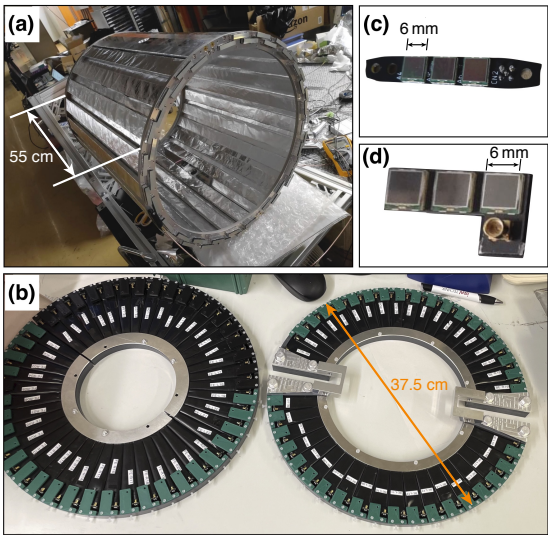

Fig. 3. Pictures of the newly developed plastic scintillators PSB (a), PSFE (left in panel (b)), and PSBE (right in panel (b)). Panels (c) and (d) show the circuit boards with MPPCs (Hamamatsu Photonics, S13360-6050PE) for PSB and for PSFE and PSBE, respectively.

2.2. Data collection

We have successfully collected data for both experiments performed in 2022. Particle-selective signals provided by the detectors on the FRS side triggered the whole data acquisition system, which enabled us to efficiently accumulate data of the reactions of interest. In the η'-mesic nuclei experiment, we recorded $\sim 1 \times 10^7$ events of the ^{12}C(p,d) reaction in a 62-hour data collection time. In the HypHI experiment, we obtained $\sim 3 \times 10^8$, 1×10^8, and 2×10^8 events with ^{3}He, ^{4}He, and d at the FRS-F4 focal plane, respectively, in 85-hour data accumulation with a 1.96 GeV/u ^{6}Li beam.

3. Status of data analysis

The data analysis is currently in rapid progress. Here, we present some of the preliminary results from the detector analysis to demonstrate that all the detector components were operated and functioning in good condition.

First, the particle identification at FRS-F4 in the η'-mesic nuclei experiment is shown in Fig. 4. The upper left panel is a time-of-flight (TOF) spectrum between SC31 and SC41 with SC41 triggering the data acquisition system, which is dominated by a large amount of proton background. Thus, we constructed and utilized a deuteron-selective trigger based on TOF(SC31-SC41) for the main data collection. As shown in the lower left panel, the deuteron trigger rejected most of the proton background, while accidental two-proton events are still remaining. Such an accidental background can be further rejected in the TOF analysis in different sections like TOF(SC41-SC43), as displayed in the right panel.

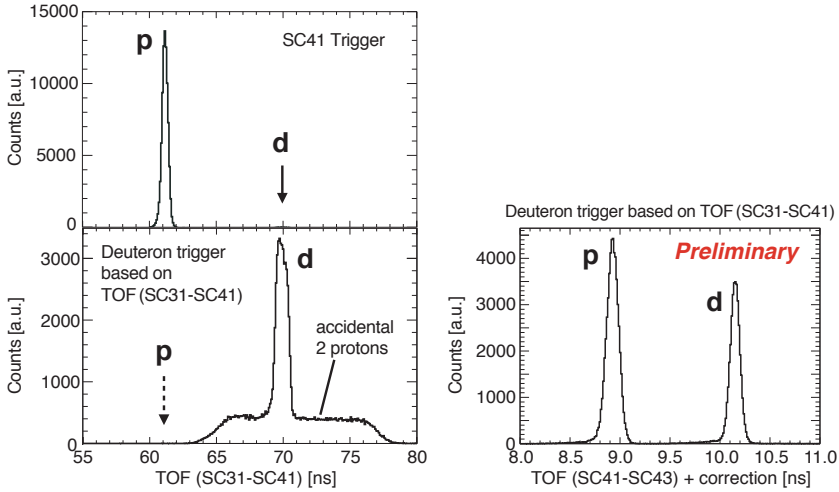

Fig. 4. Left: TOF spectra between SC31 and SC41 obtained with the SC41 trigger (upper panel) and with the TOF-based deuteron-selective trigger (lower panel). Right: TOF between SC41 and SC43 with corrections for the position and the angle of particles at F4.

Similarly, an example of particle identification at F4 during the HypHI experiment is shown in Fig. 5 for the FRS setting for ^{4}He and deuterons. Only ^{4}He and deuterons reached F4 in this setting. Since they have nearly identical TOF values, information on the energy deposition in the scintillators, such as SC42 shown in the figure, is mainly used for their identification.

Next, data from the detectors at F2 are analyzed to identify light decay particles, particularly π^- in the HypHI experiment and protons in the η'-mesic nuclei experiment. Hits recorded by MDC, PSB, PSBE, PSFE, and MFTs are used to reconstruct the tracks of the charged particles in the magnetic field and thereby their momenta. We employ the Kalman filter algorithm with the GENFIT tracking toolkit [28, 29]. Furthermore, the in-

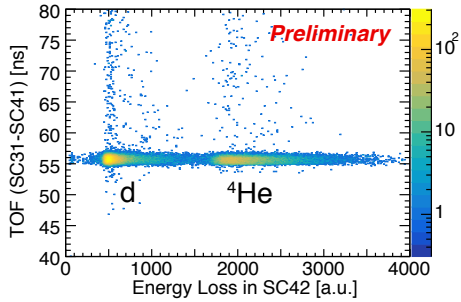

Fig. 5. Particle identification plot with the FRS setting for ^{4}He and deuteron during the HypHI experiment. The abscissa shows energy deposition measured by SC42, and the ordinate shows TOF between SC31 and SC41.

formation on the particle velocity can be obtained by the TOF between the start counter and the PSB or PSFE especially with the HypHI configuration or by the energy deposition in PSB, PSBE, or PSFE. The performance of the newly-constructed PSB has been self-checked by analyzing TOF between two adjacent overlapping segments of PSB, as shown in Fig. 6. The achieved TOF resolution is ~ 100 ps (σ), corresponding to the time resolution of single PSB ~ 70 ps (σ).

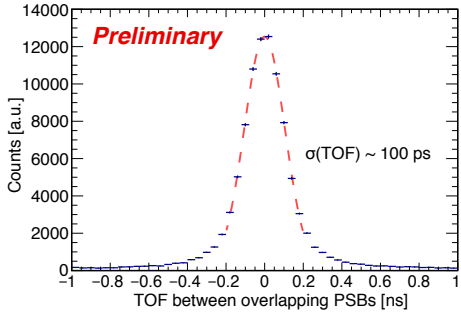

Fig. 6. (Color online) TOF between two overlapping segments of the PSB. The red dashed curve shows a fit with a Gaussian function.

Finally, a preliminary particle identification plot is shown in panel (a) of Fig. 7 with the data from the HypHI experiment [30]. We can clearly observe concentrations for π^-, π^+, and proton in the correlation plot between the momentum times charge and the velocity β. A similar analysis is in progress for the data of the η'-mesic nuclei experiment. In panel (b) of Fig. 7, we plot also a correlation between the energy deposition in SEC and that in PSB for charged particles. There are two clusters observed in this plot, which can be assigned to protons and pions, by comparing them with simulated distributions, for example, given in Ref. [31].

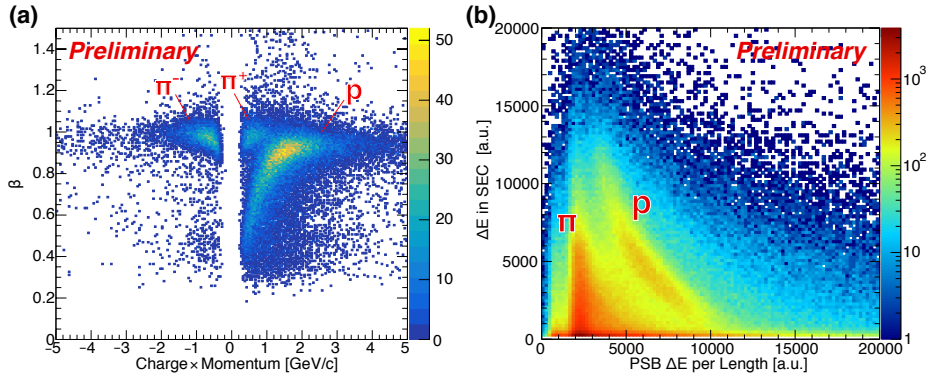

Fig. 7. (a) A preliminary plot of particle identification with WASA at F2 in the HypHI experiment. The abscissa shows the momentum times charge, and the ordinate shows the velocity normalized to the speed of light (β). This plot is based on Ref. [30]. (b) Correlation between the energy deposition ΔE in the SEC and that in the PSB with data from the η'-mesic nuclei experiment. Only 6% of the total CsI crystals are used for this preliminary plot.

4. Summary

We have developed a new experimental setup combining the WASA central detector with the fragment separator FRS at GSI. This unique setup enables coincidence measurements of forward particles with an excellent momentum resolution by the FRS and decay particles emitted in a wide angular range by the WASA detector system. We successfully performed two experiments, the spectroscopy experiment of η'-mesic nuclei and the HypHI experiment, in the first WASA-FRS campaign in 2022. Proper functionality of the detector system for the coincidence measurements has been demonstrated already by the preliminary data analysis. Further analyses for both of the two experiments are in progress.

The authors would like to acknowledge the GSI staff for their support in the experiment. This work is partly supported by the JSPS Grants-in-Aid for Early-Career Scientists (grant No. JP20K14499) and for Scientific Research (B) (grant No. JP18H01242), JSPS Fostering Joint International Research (B) (grant No. JP20KK0070). The authors would like to acknowledge support from the SciMat and qLife Priority Research Areas budget under the program Excellence Initiative-Research University at the Jagiellonian University, from Proyectos I+D+i 2020 (ref: PID2020-118009GA-I00), from the program 'Atracción de Talento Investigador' of the Community of Madrid (grant 2019-T1/TIC-131), the Regional Government of

Galicia under the Postdoctoral Fellowship Grant No. ED481D-2021-018, the MCIN under grant No. RYC2021-031989-I, and from the European Union's Horizon 2020 research and innovation programme (grant No. 824093).

REFERENCES

[1] T. Yamazaki *et al.*, *Phys. Rep.* **514**, 1 (2012).
[2] R.S. Hayano, T. Hatsuda, *Rev. Mod. Phys.* **82**, 2949 (2010).
[3] D. Gotta, *Prog. Part. Nucl. Phys.* **52**, 133 (2004).
[4] V. Metag, M. Nanova, E.Ya. Paryev, *Prog. Part. Nucl. Phys.* **97**, 199 (2017).
[5] S.D. Bass, P. Moskal, *Rev. Mod. Phys.* **91**, 015003 (2019).
[6] D.H. Davis, *Nucl. Phys. A* **754**, 3 (2005).
[7] R.H. Dalitz, *Nucl. Phys. A* **754**, 14 (2005).
[8] O. Hashimoto, H. Tamura, *Prog. Part. Nucl. Phys.* **57**, 564 (2006).
[9] A. Feliciello, T. Nagae, *Rep. Prog. Phys.* **78**, 096301 (2015).
[10] C. Bargholtz *et al.*, *Nucl. Instrum. Methods Phys. Res. A* **594**, 339 (2008).
[11] WASA-at-COSY Collaboration (H.-H. Adam *et al.*), arXiv:nucl-ex/0411038.
[12] H. Geissel *et al.*, *Nucl. Instrum. Methods Phys. Res. B* **70**, 286 (1992).
[13] K. Itahashi *et al.*, Experimental Proposal to FAIR Phase-0 at GSI, S490 (2019).
[14] T.R. Saito *et al.*, Experimental Proposal to FAIR Phase-0 at GSI, S447 (2019).
[15] H. Nagahiro, S. Hirenzaki, *Phys. Rev. Lett.* **94**, 232503 (2005).
[16] H. Nagahiro, M. Takizawa, S. Hirenzaki, *Phys. Rev. C* **74**, 045203 (2006).
[17] S. Sakai, D. Jido, *Phys. Rev. C* **88**, 064906 (2013).
[18] S.D. Bass, A.W. Thomas, *Phys. Lett. B* **634**, 368 (2006).
[19] D. Jido, H. Nagahiro, S. Hirenzaki, *Phys. Rev. C* **85**, 032201(R) (2012).
[20] H. Nagahiro *et al.*, *Phys. Rev. C* **87**, 045201 (2013).
[21] Y.K. Tanaka *et al.*, *Phys. Rev. Lett.* **117**, 202501 (2016).
[22] Y.K. Tanaka *et al.*, *Phys. Rev. C* **97**, 015202 (2018).
[23] N. Tomida *et al.*, *Phys. Rev. Lett.* **124**, 202501 (2020).
[24] C. Rappold *et al.*, *Phys. Rev. C* **88**, 041001 (2013).
[25] C. Rappold *et al.*, *Nucl. Phys. A* **913**, 170 (2013).
[26] R. Ruber, Ph.D. Thesis, Uppsala University, 1999.
[27] R. Sekiya *et al.*, *Nucl. Instrum. Methods Phys. Res. A* **1034**, 166745 (2022).
[28] C. Höppner *et al.*, *Nucl. Instrum. Methods Phys. Res. A* **620**, 518 (2010).
[29] T. Bilka *et al.*, arXiv:1902.04405 [physics.data-an].
[30] H. Ekawa *et al.*, *EPJ Web of Conf.* **271**, 08012 (2022).
[31] W. Krzemień, Ph.D. Thesis, Jagiellonian University, 2011, arXiv:1202.5794 [nucl-ex].